AUTOMATED DYNAMIC MODE MULTIDIRECTIONAL UV LITHOGRAPHY FOR COMPLEX 3-D MICROSTRUCTURES

Jungkwun Kim[1], Mark G. Allen[2] and Yong-Kyu 'YK' Yoon[1]
[1]University at Buffalo, the State University of New York, Buffalo, NY, USA
[2]Georgia Institute of Technology, Atlanta, GA, USA

ABSTRACT

Automated multidirectional UV exposure has been demonstrated using a collimated UV source and a movable stage equipped with two computer controlled motors and a microcontroller for complex three dimensional (3-D) microstructures. The stage is tilted and rotated using independently controlled motors during UV exposure as programmed by the user. Various dynamic operations with the synchronized angular velocities of tilting and rotation have been performed using an SU-8 substrate and a reverse-side exposure scheme. Fabricated structures using the dynamic mode include a vertical reverse triangular slab, a quadruple reverse triangular slab, a cardiac horn, screwed wind vane shapes with double blades and quadruple blades. Ray tracing simulation using mathematical equations has been performed to analytically confirm the shapes of resultant structures.

Index Terms—Automated UV exposure, Inclined exposure, multidirectional UV lithography, rotational exposure, screwed wind vane.

1. INTRODUCTION

One of the most commonly used methods to fabricate three dimensional (3-D) MEMS structures is ultraviolet (UV) lithography since the equipment utilized in UV lithography is relatively inexpensive compared to that of the X-ray or laser process [1-3]. Since the photopatternable, negative-tone epoxy resin SU-8 was introduced in the mid-1990s, SU-8 has been very widely used to fabricate 3-D structures with very high-aspect-ratio geometries using UV or near-UV light sources [4-6].

Recently, multidirectional UV lithography using SU-8, where the UV source and a substrate have an arbitrary angle rather than having a perpendicular position to each other as in the conventional UV lithography, has been introduced. This approach is attractive for complex 3-D microfabrication due to fabrication simplicity, cost effectiveness, and manufacturability [7-10]. Examples include a vertical screen microfluidic filter structure, a mixer, and micronozzle and horn arrays [7, 10]. However, the previous exercises have been limited to either a purely static mode, in which the tilted stage is fixed during each UV exposure or a partial dynamic mode, in which the tilted angle is fixed while the stage keeps rotating in a constant speed producing axisymmetric structures.

In this work, the fully computer controlled dynamic mode multidirectional UV exposure scheme has been demonstrated, where the substrate holding stage is independently controlled for tilting and rotating during UV exposure as programmed by the user. Unusual 3-D microstructures with non-axisymmetric curved sidewalls such as a cardiac shaped horn and screwed wind vanes with double and quadruple blades are demonstrated. The automated system has tilting and rotational angles and their angular velocities as design variables, and ray tracing simulation with analytical equations with those variables has been performed to confirm the experimental results.

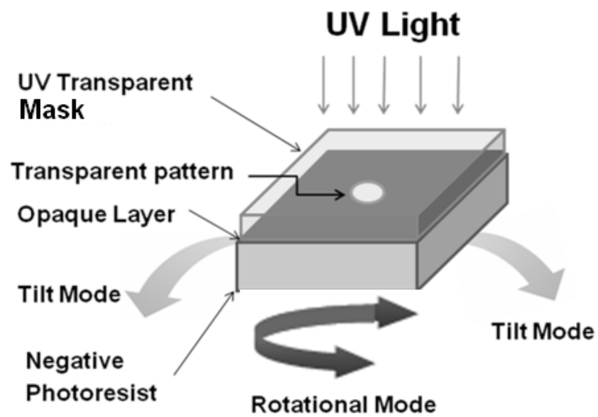

Figure 1: Dynamic mode multidirectional UV exposure

2. AUTOMATED DYNAMIC MODE MULTIDIRECTIONAL UV LITHOGRAPHY

In contrast to conventional UV lithography, where the incident light is perpendicular to the substrate plane, multidirectional UV lithography employs an arbitrary incident angle between 0° and 90° from the vertical line of the photomask and substrate plane [7]. The arbitrary angle would be achieved either by a fixed substrate and a movable exposure light head, or by a fixed light head and a movable substrate stage. The latter is considered as a more economic way when a pre-existing UV source is used in a prototyping environment.

The movable stage has two degrees of freedom as shown in Figure 1: tilting and rotation. Dynamic mode operation involves the discrete or continuous movement of the stage during UV exposure. The tilting and rotation movement in this work is automated by programming.

Figure 2: shows the system apparatus consisting of a collimated UV light source (LS 30, OAI Inc.), a dynamic stage with two degrees of freedom for tilting and rotation, and a stage controlling computer. The light source produces intense, uniform, collimated UV with a wavelength of 365nm. The stage is equipped with two stepper motors (MD-2A, Arrick Robotics, Inc.) and is controlled by computer.

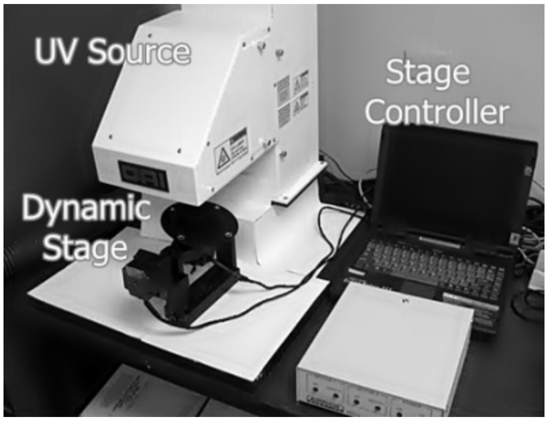

Figure 2: System apparatus

3. FABRICATION PROCESS

The fabrication process is shown in Figure 3. A chromium-coated glass plate is used as a substrate. After patterning chromium for UV incidence, SU-8 is coated on the substrate to a thickness which will ultimately define the height of the structure. After the SU-8 is baked, the substrate is turned over and exposed at different angles where the tilting and rotational angles are dynamically changing during UV exposure as the user programmed (Figure 3a, 3b). Exposure is followed by a post-exposure bake to cross-link SU-8. A develop step then reveals complete projected structures (Figure 3c). A fabricated sample structure is shown in Figure 3d.

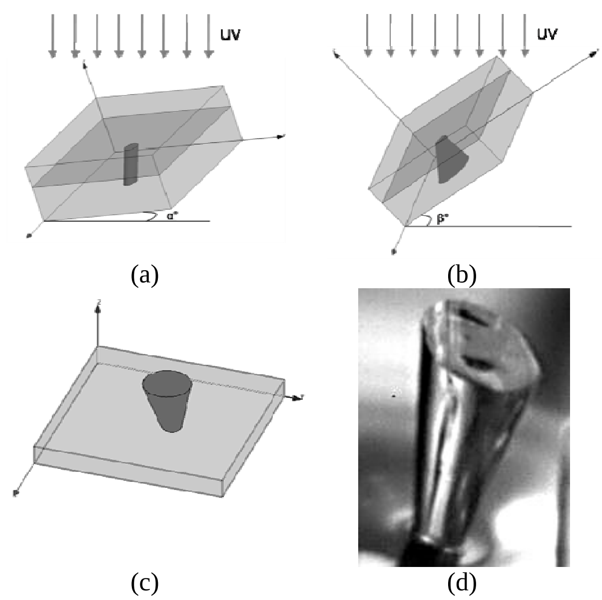

Figure 3: Fabrication process: (a) Expose the sample with a tilting angle of α°, (b) Change the tilting angle with continuous rotation during exposure, (c) Post exposure bake and develop to complete the process, (d) Fabricated asymmetric corn structure

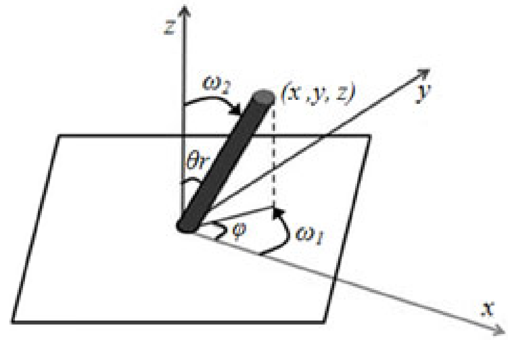

Figure 4: Coordinate system used for structural simulation

4. AUTOMATION ALGORITHM

The tilting and rotational motion can be controlled in a synchronous or asynchronous mode. The synchronous mode operation can utilize various mathematical functions to correlate the tilting motion to the rotating motion. To describe their ray trace simulation mathematically, a polar coordinate system is adopted as shown in Figure 4 [7]. The refracted light in the polymeric slab through a clear window of a dark field photomask is described using a spherical coordinate system (*x,y,z*), where θr is the refracted angle from the axis (the latitudinal angle) and is controlled by a tilting motion, and φ is the angle from the x axis in the x-y plane (the longitudinal angle) and is controlled by a rotational motion.

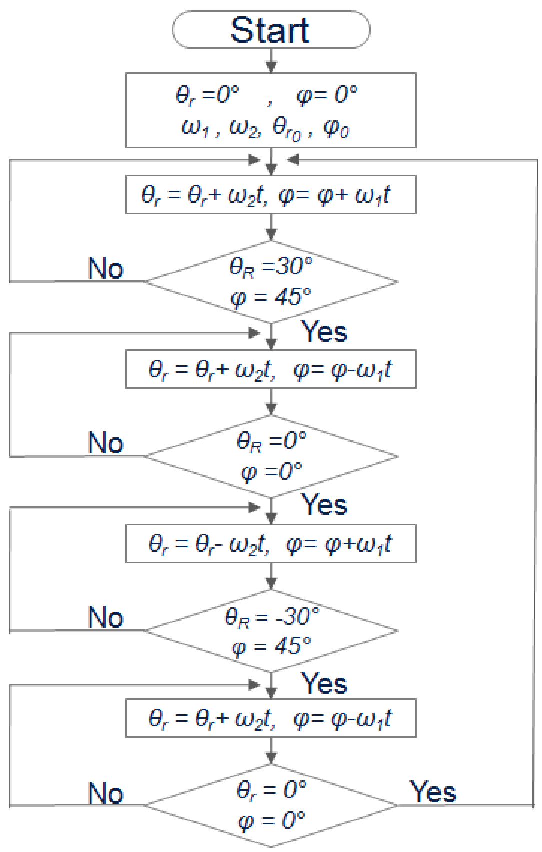

Figure 5: Automated dynamic mode operation algorithm for a screwed wind vane

Pattern	**(a) Vertical reverse triangular slab**	**(b) Quadruple triangular slab**	**(c) Cardiac horn**	**(d) Screwed wind vane with double blades**	**(e) Screwed wind vane with quadruple blades**
Refracted angle	$-30° < \theta < 30°$	$-30° < \theta < 30°$	$-3 < \theta < 30°$ $\theta = \theta r_0 \cos\omega_2 t$	$-30° < \theta < 30°$ $\theta = \theta r_0 \cos\omega_2 t$	$-30° < \theta < 30°$ $\theta = \theta r_0 \cos\omega_2 t$
Angle	$\varphi=0$	$\varphi= 0, 90°$	$\varphi = \omega_1 t$	$0 < \varphi < 45°$ $\varphi = \lvert\omega_1\rvert t$	$0 < \varphi < 45°$, $90° < \varphi < 135°$ $\varphi = \lvert\omega_1\rvert t, 90° + \lvert\omega_1\rvert t$
3-D Ray trace			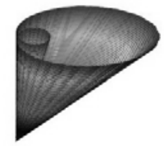		
Fabricated structures	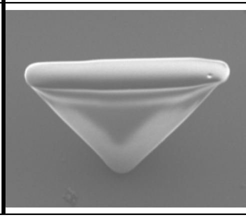	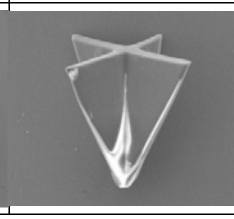	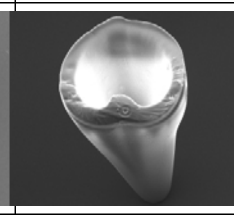	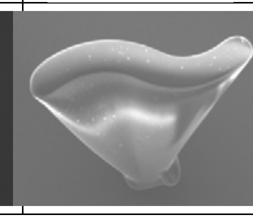	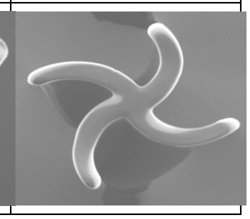

Table 1: Dynamic mode multidirectional UV lithography with a continuously varying rotational and tilting substrate

In this work, the synchronous mode dynamic operation is considered, where the rotational angular velocity ω_1 and the tilting angular velocity ω_2 are harmonically related. Given those four variables (φ, θr, ω_1, and ω_2), an example of operation algorithm for a screwed wind vane is shown in Figure 5.

Using the same coordinate system, 3-D ray tracing with the variables of φ, θr, ω_1, ω_2 is also performed using the mathematical software, MathCAD. Since the two motors are independently controlled the rotating and tilting movement can show an infinite number of motions individually or by combination.

5. RESULT

As an example of the rotational and tilting functions, a constant angular velocity ω_1 is used for the rotational movement ($\varphi = \omega_1$ t, where t is time) while a cosine function with a maximum refraction angle of θr_0 and an angular velocity of ω_2 is used for the tilting movement ($\theta = \theta r_0 \cos \omega_2 t$)). The (x, y, z) position is described as Eqs (1), (2), and (3), respectively.

$$x = z\tan(\theta_{r_0}\cos\omega_2 t)\cos\omega_1 t \quad (1)$$
$$y = z\tan(\theta_{r_0}\cos\omega_2 t)\sin\omega_1 t \quad (2)$$
$$z = z \quad (3)$$

where θr_0 is the maximum refracted angle, ω_1 the angular velocity of the rotating motion, and ω_2 the angular velocity of the tilting motion.

Some examples fabricated using the different tilting and rotational angles and angular velocities are shown in Table 1. A single hole and hole array are used as mask patterns. The vertical reverse triangular slab is shown in the first column where the refracted angle is varied from -30° to +30° with no rotation. Note the tilting angle for the stage is approximately 75° to achieve the resultant angle of 30° taking into account the refractive index difference between SU-8 and air [7]. A quadruple reverse triangular slab is fabricated similarly with two discrete longitudinal angles φ of 0° and 90°. As an example of an asymmetric complex structure, a cardiac horn is demonstrated in the third column. With an initial tilting angle of -5°, the stage is dynamically tilted to 75° in an angular velocity of ω_2 while rotating in a constant angular velocity of ω_1 in a synchronous mode with both ω_1 and ω_2 of 20rpm until the desired dose is supplied to the SU-8. The resultant refracted angle is reduced due to the refracted index of refraction difference.

More complex 3-D structures are also demonstrated such as screwed wind vanes with double blades and quadruple blades in the fourth and fifth column, respectively. For the screwed wind vane with double blades, the tilting angle is moving from -75° and +75° with an angular velocity of ω_2 while the rotational angle is changing back and forth between 0° and 45° with an angular velocity ω_1. Again both angular velocities ω_1 and ω_2 are the same of 20rpm in this case. For the quadruple blades, the process is repeated with a longitudinal angle offset of 90° after exposure for the screwed wind vane with double blades is performed. An array mask can produce array structures as shown in Figure 6.

Also, the ray tracing simulation has been performed using Eqs (1), (2), and (3) and MathCAD the schematics are added in Table 1. The overall shapes of the fabricated structures and the simulated ones show good agreement. Their parasitic effects due to diffraction, refraction, and overexposure are not considered in this simulation. Also note that the beam thickness is not taken into account for the simulation. However, this simple ray tracing simulation provides a useful guideline for more 3-D challenging pattern design.

6. CONCLUSION

We have demonstrated automated dynamic mode multidirectional UV lithography and produced various complex structures from a single and array mask pattern. Dynamic mode UV lithography has additional process parameters, such as tilting angle, rotational angle, their angular velocities, and synchronization between inclined and rotational motions, in addition to main parameters in the static mode multidirectional UV exposure such as tilting angle, refractive index of photoresist, and thickness of photoresist. By combining and varying these parameters, a variety of complex 3-D structures would be produced. To demonstrate the versatile 3-D fabrication capability of this process, a vertical reverse triangular slab, a vertical reverse quadruple triangular slab, a cardiac horn, a screwed wind vanes with two blades and four blades are fabricated. Ray tracing simulation has been performed using mathematical equations and MathCAD. The shapes of the fabricated structures and the simulated ones agree very well. These kind of 3-D structures will find large potential for RF applications such as integrated millimeter-wave and terahertz antennas and waveguides, as well as microfluidic applications such as rotors and microturbines.

ACKNOWLEDGEMENTS

The authors thank Sungyong Cha for the ray tracing simulation of the 3-D microstructures and Myounggu Kang and Jungwoo Song for their technical support of SEM pictures in the University at Buffalo.

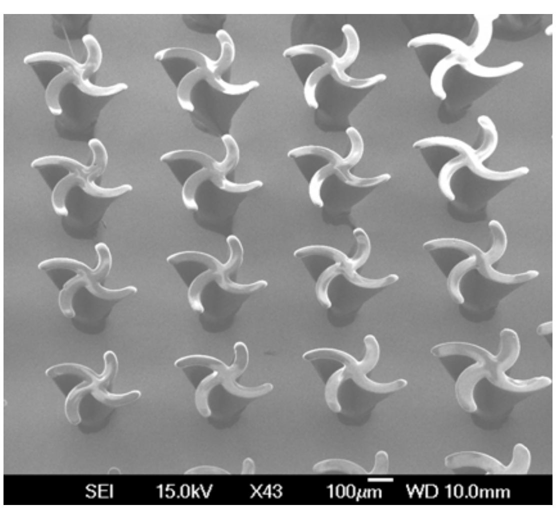

Figure 6: SEM Photograph of the 3-D microstructure array fabricated using automated dynamic mode multidirectional UV lithography

REFERENCES

[1] W. Ehrfeld, F. Gotz, D. Munchmeyer, W. Schelb, and D. Schmidt, "LIGA process: Sensor construction techniques via X-ray lithography," in Proc. Solid-State Sens. Actuator Workshop, Hilton Head Island, SC, 1988, pp. 1–4.

[2] P. Bley, J. Gottert, M. Harmening, M. Himmelhaus, W. Menz, J. Mohr, C. Muller, and U. Wallrabe, "The LIGA process for the fabrication of micromechanical and mirooptical components," in Micro System Technologies, Berlin, Germany, 1991, pp. 302–314.

[3] G. P. Behrmann and M. T. Duignan, "Excimer laser micromachining for rapid fabrication of diffractive optical elements," Appl. Opt., vol. 36, pp. 4666–4676, 1997.

[4] H. Lorenz, M. Despont, N. Fahrni, N. LaBianca, P. Renaud, and P. Vettiger, "SU-8: A low-cost negative resist for MEMS," J. Micromech. Microeng., vol. 7, pp. 121–124, 1997.

[5] F. Cros and M. G. Allen, "High aspect ratio structures achieved by sacrificial conformal coating," in Proc. Solid-State Sensor and Actuator Workshop, Hilton Head Island, SC, 1998, pp. 261–264.

[6] J. Zhang, K. L. Tan, G. D. Hong, L. J. Yang, and H. Q. Gong, "Polymerization optimization of SU-8 photoresist and its applications in microfluidic systems and MEMS," J. Micromech. Microeng., vol. 11, pp. 20–26, 2001.

[7] Y.-K. Yoon, J.-H. Park, and M.G. Allen, "Multidirectional UV lithography for complex 3-D MEMS Structures," IEEE Journal of MEMS, vol. 15, no. 5. October 2006

[8] H. Sato, T. Kakinuma, J. S. Go, and S. Shoji, "In-channel 3-D Micromesh Structures using Maskless Multi-Angle Exposures and their Microfilter Application", Sensors and Actuators A, 111 (2004), pp. 87-92.One of Shoji papers

[9] M. Han, W. Lee, S.-K. Lee, and S.S. Lee, "Fabrication of 3D microstructures with inclined/rotated UV lithography," Proceedings of IEEE Micro Electro Mechanical Systems, 2003, pp. 554-557.

[10] Yong-Kyu Yoon and M.G. Allen, "Proximity Mode Inclined UV Lithography," Solid-State Sensor, Actuator, and Microsystems Workshop, Hilton Head Island, SC, June 4-8, 2006, pp. 98 – 99